SUPPLEMENTARY TABLES

Supplementary Table 1. The number of lipid species identified in positive and negative ion MS modes using 4 different lipid extractions of a mouse brain.

Extraction Method	# Lipid species (positive mode)	# Lipid species (negative mode)	# Lipid species (both modes)
Folch	232	129	361
Folch - HCl	316	189	**505**
Bligh Dyer	362	222	584
Bligh Dyer - HCl	497	324	**821**

Supplementary Table 2. Results from untargeted LC-MS analyses (ddMS2) to identify lipids that were significantly altered upon overexpression of recombinant DGKε in HEK293T cells (*n*=5 biological samples). Significantly altered lipids were identified by a Q-value < 0.05 following a Benjamini-Hochberg correction of a two-sided binomial test. Data shown are representative of two experiments (*n*=2 biologically independent experiments).

Lipid ID	Log_2 Fold Change	Q Value
PG(18:1/14:0)	2.03	0.0001
TG(18:1/18:1/20:4)	-2.38	0.0002
PI(16:0_20:4)	**1.89**	**0.0003**
PG(16:1/18:1)	-1.15	0.0003
PE(18:1/20:4)	-0.47	0.0006
PS(16:0/20:4)	-3.07	0.0015
PG(18:1/18:1)	-0.68	0.0037
PE(16:1/18:1)	-0.26	0.0146
PE(18:2/22:6)	-0.31	0.0161
PG(18:0/18:1)	-0.26	0.0247
PG(18:1/20:4)	0.97	0.039
PC(18:0/18:1)	-0.27	0.041
PC(18:1/18:1)	-0.33	0.041
PE(16:1/22:6)	-0.38	0.041
PI(18:0/22:6)	2.12	0.041
PS(18:0/22:4)	-0.56	0.041
SM(d16:1/18:1)	-0.39	0.041
PE(16:1/16:1)	-0.34	0.0418
SM(d18:0/18:1)	-0.36	0.0418
PA(16:0/16:0)	1.33	0.0058

Supplementary Table 3. DAG lipids with cellular levels that were reduced upon recombinant overexpression of DGKα in HEK293T cells (*n*=5 biological samples). The fatty acid composition of lipids shown match DAG species identified as substrates of endogenous DGKα in A549 shRNA-mediated knockdown studies (Supplementary Fig. 14). Data shown are representative of two experiments (*n*=2 biologically independent experiments).

Lipid ID	Log_2 Fold Change
C18:0_18:0 DAG	-0.17
C18:1_20:1 DAG	-0.21
C16:0_22:1 DAG	-0.20
C16:1_18:1 DAG	-0.19
C16:0_20:1 DAG	-0.25

SUPPLEMENTARY FIGURES

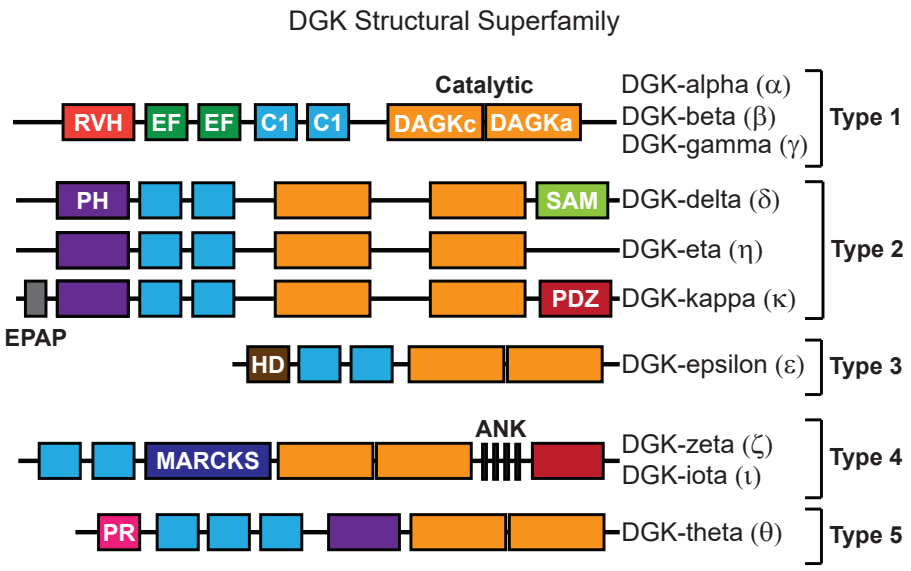

Supplementary Figure 1. **The diacylglycerol kinase superfamily regulates cell signaling via metabolism of lipid messengers**. Classification of the 10 mammalian DGK isoforms into 5 subtypes based on structural motifs. RVH: recoverin homology domain; EF: EF Hand motif; C1: atypical/typical C1 domain; PH: pleckstrin homology domain; SAM: sterile alpha motif; EPAP: Glu-Pro-Ala-Pro repeats; PDZ: protein-protein interactions; HD: hydrophobic domain; MARCKS: myristoylated alanine rich protein kinase C substrate domain; ANK: Ankyrin repeats; PR: proline-rich region.

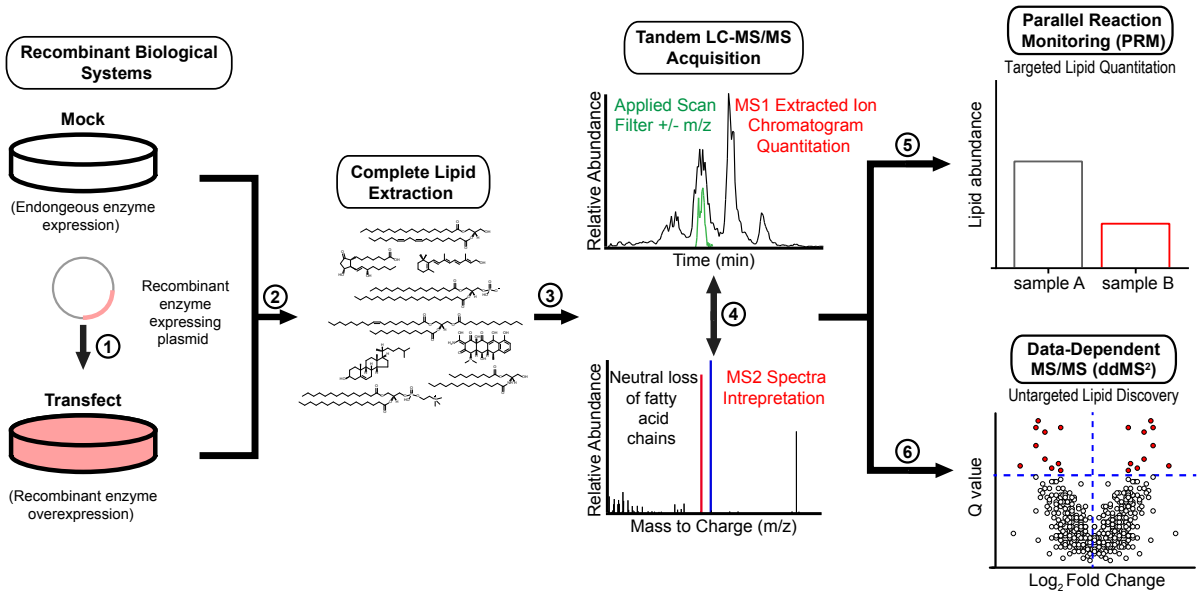

Supplementary Figure 2. **Metabolomics platform for quantitative evaluation of the DGK-regulated lipidome**. Evaluation of DGK metabolic activity in live cells was achieved by: (1) recombinant overexpression of individual DGK isoforms via transient transfection. (2) Lipid extraction using a modified Bligh Dyer method. (3) Quantitative analysis of cellular lipids using tandem LC-MS/MS for the separation of lipids and subsequent detection of MS1 precursor ions and MS2 fragment ions. (4) Lipid identification using LipidSearch™, which matched MS1 and MS2 ions with library spectra, followed by quantitation of lipid abundance by peak area. Diagnostic ions (i.e. loss of fatty acid chains) were used to distinguish closely related lipid species. (5) Parallel-reaction monitoring (PRM) for targeted quantitation of changes in low abundance and/or co-eluting lipid species. (6) Top10 data-dependent method (i.e. ddMS2) to acquire MS2 spectra for the 10 most abundant ions from each MS1 scan event for discovery-based, global lipidome profiling. Mock data shown in workflow (5, 6) are representative of analyses performed using LC-MS/MS.

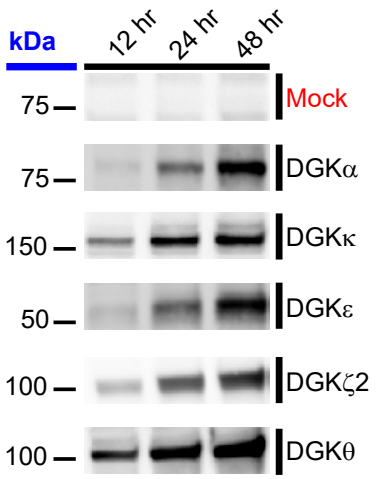

Supplementary Figure 3. **Time-course of recombinant overexpression of mammalian DGK isoforms in HEK293T cells**. Western blots showing the expression of a representative human DGK isoform from each subtype over a 48-hour time course after transient transfection. Recombinant DGKs were detected using anti-FLAG (DGKα, DGKκ, DGKε, DGKθ) or anti-HA (DGKζ2) antibodies. Soluble fractions are shown for DGKs except for DGKε, which is expressed in the membrane fraction. Full blot image is shown in Supplementary Fig. 25. Data shown are representative of two experiments (*n*=2 biologically independent experiments).

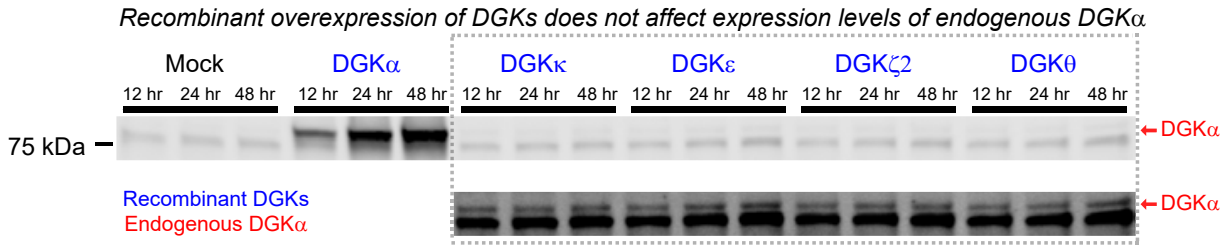

Supplementary Figure 4. **Recombinant overexpression of DGK isoforms had negligible effects on expression levels of endogenous DGKα**. Western blot showing expression levels of endogenous DGKα were not changed upon overexpression of individual recombinant human DGK isoforms in HEK293T cells over a 48-hour time course. The molecular weight (MW) of endogenous DGKα (red) matched the MW of recombinant DGKα (blue) using a polyclonal anti-DGKα antibody. The bottom panel is the same blot with enhanced contrast to highlight the endogenous DGKα band. Full blot image is shown in Supplementary Fig. 26. Data shown are representative of two experiments (n=2 biologically independent experiments).

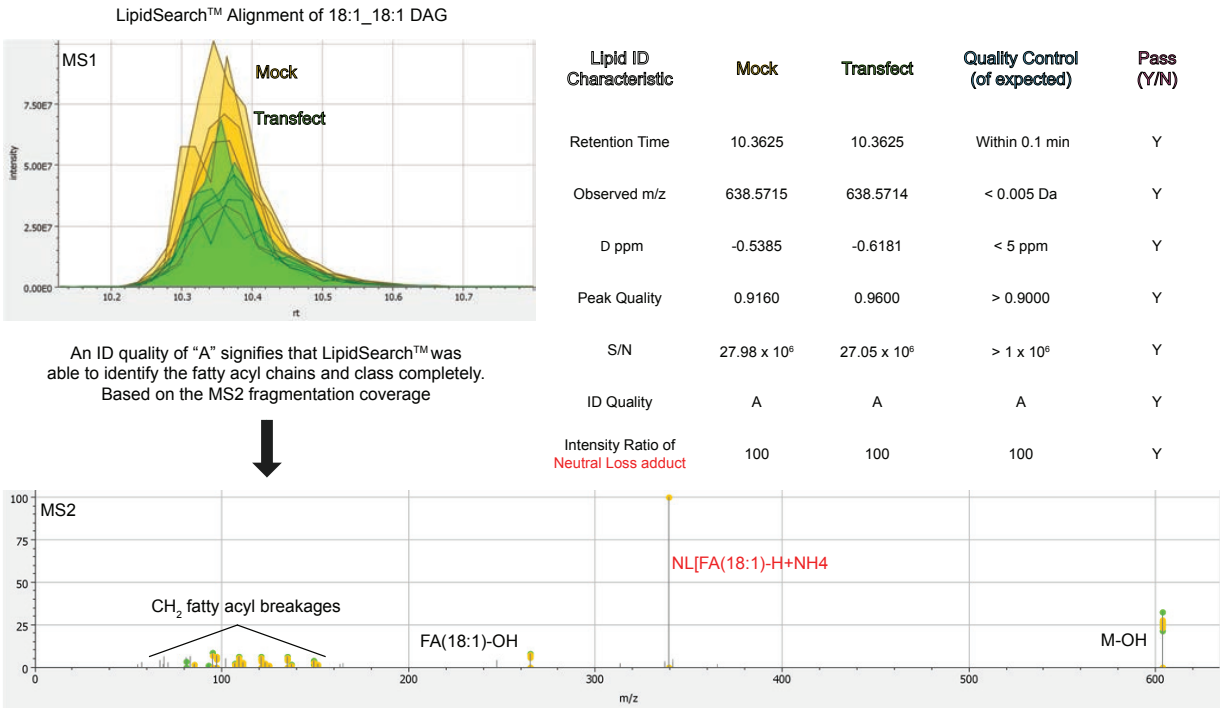

Lipid ID Characteristic	Mock	Transfect	Quality Control (of expected)	Pass (Y/N)
Retention Time	10.3625	10.3625	Within 0.1 min	Y
Observed m/z	638.5715	638.5714	< 0.005 Da	Y
D ppm	-0.5385	-0.6181	< 5 ppm	Y
Peak Quality	0.9160	0.9600	> 0.9000	Y
S/N	27.98 x 10^6	27.05 x 10^6	> 1 x 10^6	Y
ID Quality	A	A	A	Y
Intensity Ratio of Neutral Loss adduct	100	100	100	Y

Supplementary Figure 5. **Example of a manual verification to confirm lipid ion identification by LipidSearch™ software**. Lipids are identified by matching experimental MS2 spectra with in-silico spectra found in a curated database to enable identification of different classes of lipid species. The MS2 spectra are matched to precursor MS1 peaks. The MS1 area under the peak from select sample analyses can be superimposed to enable comparison of lipid levels in different samples (e.g. mock- versus DGKα-transfected HEK293T cells). High confidence lipid identifications can be obtained in LipidSearch™ through stringent stipulations of several lipid analyte detection and database match criteria: retention time, observed adduct m/z, delta ppm (mass accuracy), peak quality, signal-to-noise, ID quality, and fragment ion intensity ratios. An example MS2 spectrum is shown with annotated fragment ions typically observed in positive ion analysis of a lipid ammonium adduct ion, including loss of the hydroxyl group from precursor ion (M-OH), fragment ion resulting from the neutral loss of fatty acyl chains and ammonia (NL[FA]-H+NH_4), loss of hydroxyl group from the released fatty acyl chain (FA-OH), and multiple methylene (CH_2) loss fragmentations of these charged fatty acyl chains.

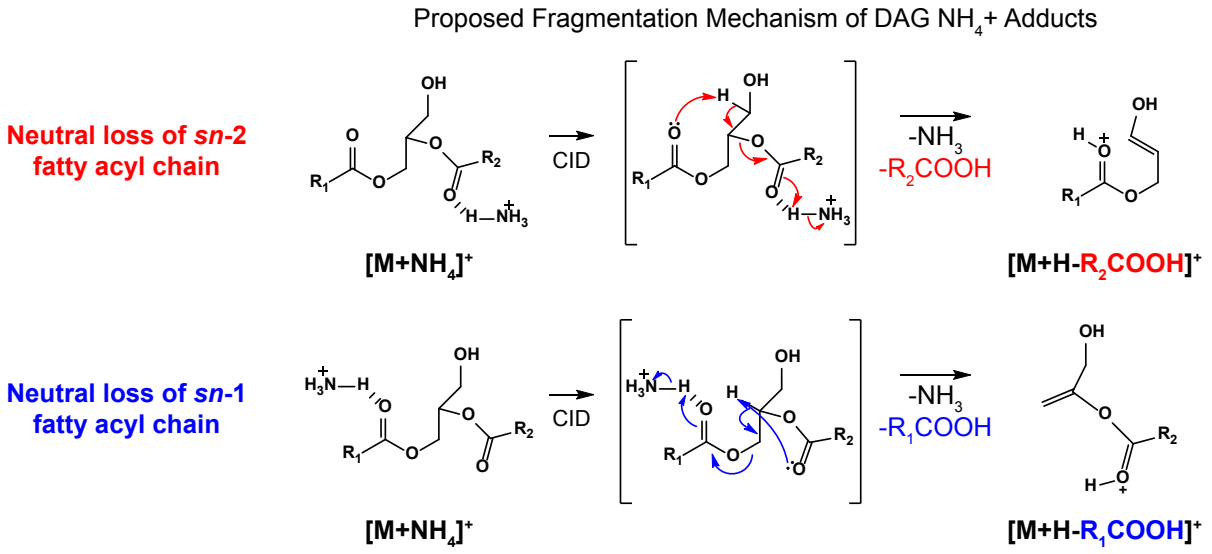

Supplementary Figure 6. HCD-induced fragmentation of ammoniated glycerolipid products. Fragmentation spectra produced by loss of ammonia and a *sn*-1 or *sn*-2 fatty acid of an ammoniated diacylglycerol (DAG) precursor ion are shown with proposed fragmentation mechanisms (red and blue peaks). All subsequent DAG identifications were confirmed by the fragment ions that resulted from the losses of both fatty acid chains from the ammoniated precursor ion.

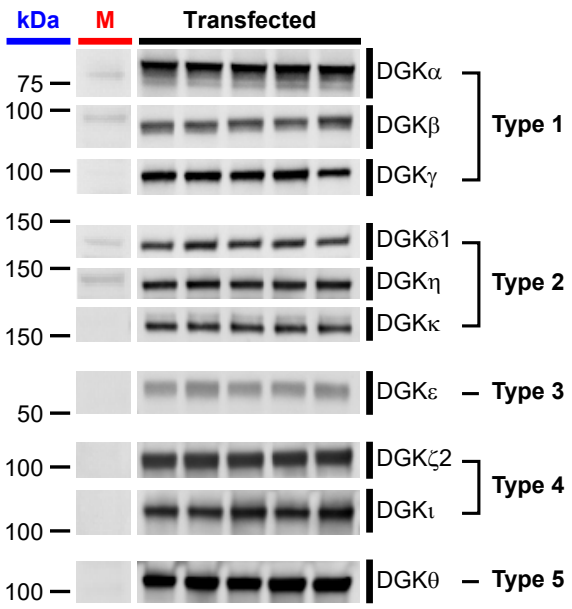

Supplementary Figure 7. **Expression of mammalian DGK isoforms in HEK293T cells**. Western blots showing recombinant overexpression of the 10 human DGK isoforms. Western blot data showed comparable expression of recombinant DGKs across 5 biological samples. All recombinant DGKs were detected using anti-FLAG antibody with the exception of DGKζ2 and DGKι, which were detected via an anti-HA antibody; "M" represents mock lane. All data shown are for soluble proteomes with the exception of recombinant DGKε, which is expressed in membrane fractions. Full blot image is shown in Supplementary Fig. 27. All data shown are representative of four experiments (*n*=4 biologically independent experiments).

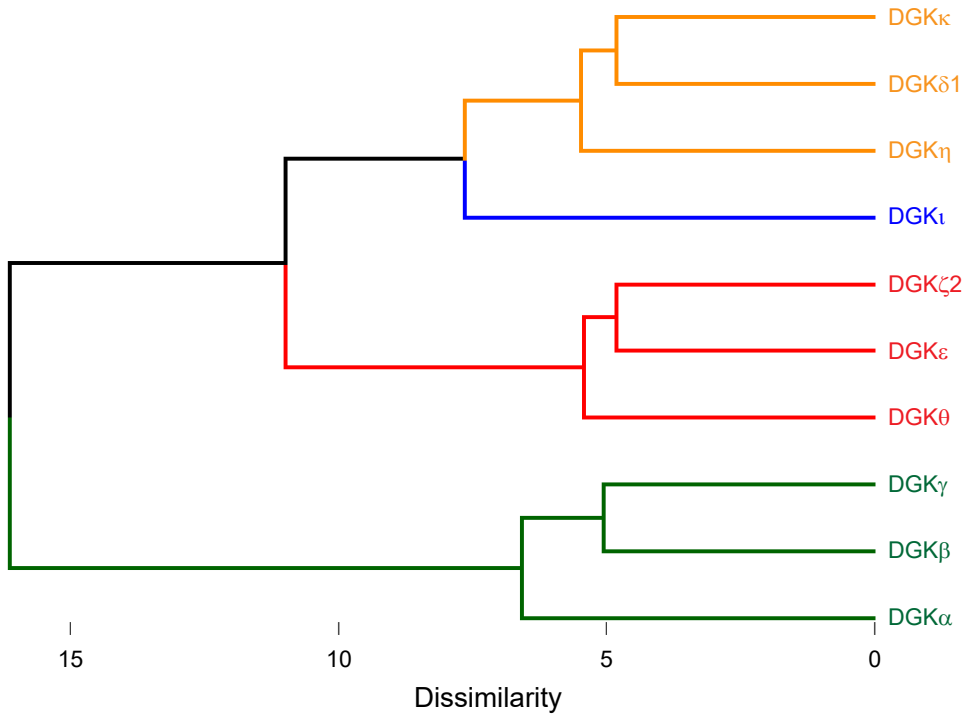

Supplementary Figure 8. Hierarchical clustering of DAG lipidome data from Fig. 2a shows relationships between DGK isoforms with regards to the magnitude of changes in detected DAGs.

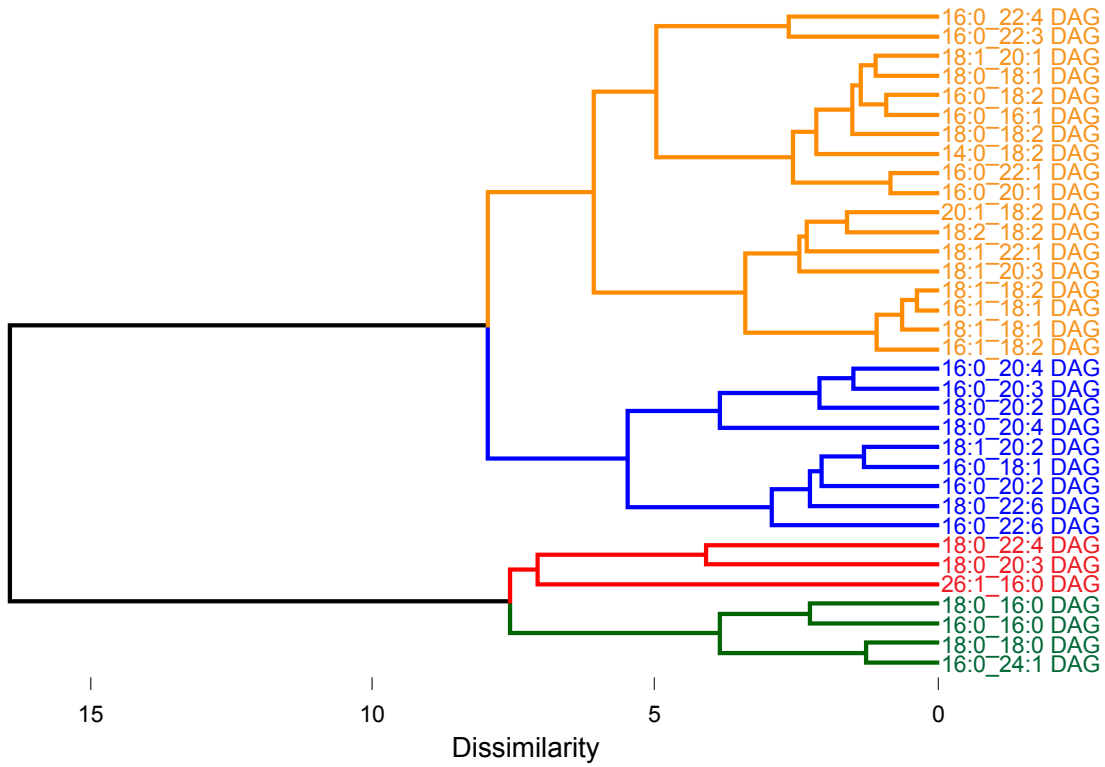

Supplementary Figure 9. Hierarchical clustering of DAG lipidome data from Fig. 2a shows the relationship for metabolism by individual isoforms (DGKα, green cluster), their fatty acyl chain composition (orange and blue clusters), or through a combination of these two relationships (red cluster).

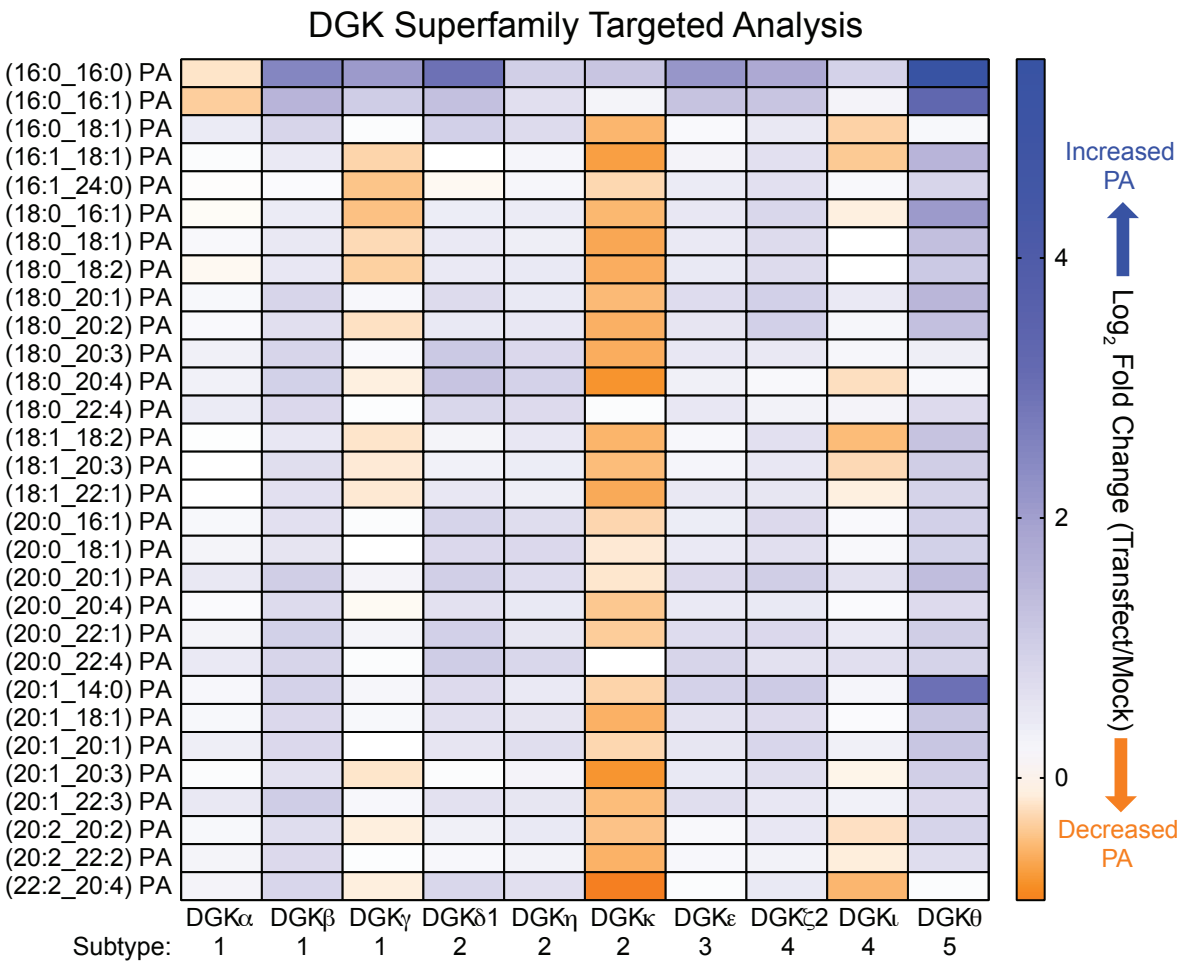

Supplementary Figure 10. **Phosphatidic acid (PA) metabolic profiles of the DGK superfamily**. Heat map displaying the $\log_2$ fold change in cellular PA lipid levels in HEK293T cells expressing individual recombinant human DGK isoforms compared with non-transfected (mock) controls (*n*=5 biological samples). Data shown are representative of two experiments (*n*=2 biologically independent experiments).

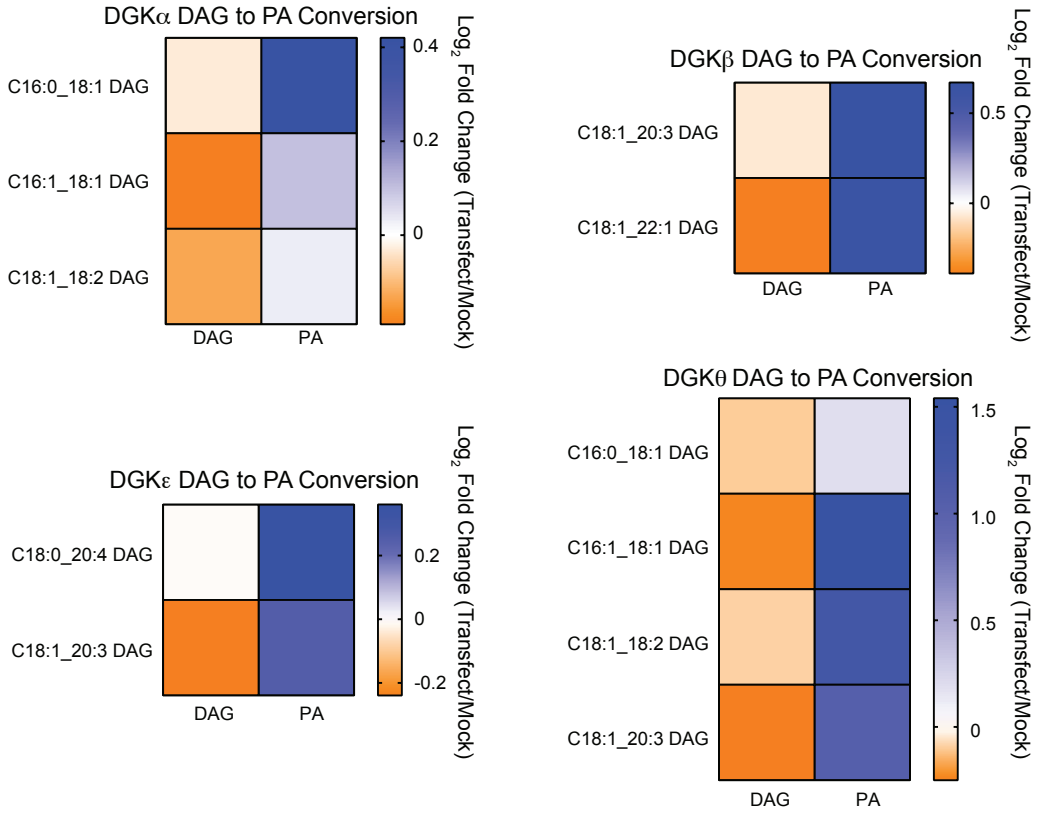

Supplementary Figure 11. **Direct DAG to PA conversion in live cells expressing recombinant DGK isoforms**. Heat maps showing DAG and PA lipids with matching fatty acyl chain composition that are decreased (blue cell) and increased (red cell), respectively, upon overexpression of recombinant human DGKs. These data support a direct DGK-mediated phosphorylation of DAG substrate to produce the corresponding PA product for the lipid compositions and DGK isoforms shown (*n*=5 biological samples). Data shown are representative of two experiments (*n*=2 biologically independent experiments).

C1A Domain

```
CLUSTAL O(1.2.4) multiple sequence alignment

DGKaC1A|P51556|203-251      HHIWRPKRFSRPVYCNLCEL-SIGLGKQGLSCNLCKYIVHDHCAMKAQPC-    251
DGKbC1A|P49621|243-292      QHVWRLKHFNKPAYCNLCLNMLIGVGKQGLCCSFCKYTVHERCARAP-PSC    292
DGKgC1A|P49620|268-318      RHAWTLKHFKKPTYCNFCHIMLMGVRKQGLCCIYCKYAVHQRCVSNSIPGC    318
                            :* *  *:*.:*.***:*    :*: ****.*  *** **::*.    *
#  Percent Identity  Matrix - created by Clustal2.1

     1: DGKaC1A|P51556|203-251  100.00   60.42   46.94
     2: DGKbC1A|P49621|243-292   60.42  100.00   62.00
     3: DGKgC1A|P49620|268-318   46.94   62.00  100.00
```

C1B Domain

```
CLUSTAL O(1.2.4) multiple sequence alignment

DGKaC1B|P51556|267-317      PHVWVRGGCHSGRCDRCQKKIRTYHSLTGLHCVWCHLEIHDDCLQAVGPEC    317
DGKbC1B|P49621|307-356      HHYWVEGNC-PTKCDKCHKTVKCYQGLTGLHCVWCQTTLHNKCASHLKPEC    356
DGKgC1B|P49620|333-380      QHAWVEGNS-SVKCDRCHKSIKCYQSVTARHCVWCRMTFHRKCELSTA--C    380
                             * **.*..   :**:*:*.:: *:.:*. *****:  :* .*       *
#  Percent Identity  Matrix - created by Clustal2.1

     1: DGKaC1B|P51556|267-317  100.00   48.00   45.83
     2: DGKbC1B|P49621|307-356   48.00  100.00   56.25
     3: DGKgC1B|P49620|333-380   45.83   56.25  100.00
```

Catalytic Domain

```
CLUSTAL O(1.2.4) multiple sequence alignment

DGKaC|P51556|365-498      SNTHPLLVFINPKSGGKQGQSVLWKFQYILNPRQVFNLK-DGPEPGLRFFKDVPQFRVLV     423
DGKbC|P49621|431-565      PGTHPLLVFVNPKSGGKQGERIYRKFQYLLNPRQVYSLSGNGPMPGLHFFRDVPDFRVLA     490
DGKgC|P49620|427-561      PGTHPLLVLVNPKSGGRQGERILQKFHYLLNPKQVFNLDKGGPTPGLNFFQDTPDFRVLA     486
                           .******::******:**: :  **:*:***:**:.*. .** ***.**:*.*:****.

DGKaC|P51556|365-498      CGGDGTVGWILETIDKANFPIVPPVAVLPLGTGNDLARCLRWGRGYEGENLRKILKDIEI     483
DGKbC|P49621|431-565      CGGDGTVGWILDCIEKANVVKHPPVAILPLGTGNDLARCLRWGGGYEGENLMKILKDIES     550
DGKgC|P49620|427-561      CGGDGTVGWILDCIDKANFTKHPPVAVLPLGTGNDLARCLRWGGGYEGGSLTKILKEIEQ     546
                          **********: *:***.   ****:**************** **** .* ****:**

DGKaC|P51556|365-498      SKVVYLDRWLLEVIP 498
DGKbC|P49621|431-565      STEIMLDRWKFEVTP 565
DGKgC|P49620|427-561      SPLVMLDRWYLEVMP 561
                          *  : **** :** *
#  Percent Identity  Matrix - created by Clustal2.1

     1: DGKaC|P51556|365-498  100.00   73.13   73.13
     2: DGKbC|P49621|431-565   73.13  100.00   77.78
     3: DGKgC|P49620|427-561   73.13   77.78  100.00
```

Accessory Domain

```
CLUSTAL O(1.2.4) multiple sequence alignment

DGKaA|P51556|512-693      QIINNYFSIGVDASIAHRFHLMREKYPEKFNSRMKNKLWYLEFATSESIFSTCKKLEESV     570
DGKbA|P49621|579-759      -IINNYFSIGVDASIAHRFHIMREKHPEKFNSRMKNKFWYFEFGTSETFSATCKKLHESV     637
DGKgA|P49620|575-749      -IMNNYFSIGVDASIAHRFHVMREKHPEKFNSRMKNKLWYFEFGTSETFAATCKKLHDHI     633
                           *:*****************:****:**********:**:**.***:: :*****.:: :

DGKaA|P51556|512-693      TVEICGKLLDLSDLSLEGIAVLNIPSMHGGSNLWGDTKRPHGDTCGINQALGSVAKIITD     630
DGKbA|P49621|579-759      EIECDGVQIDLINISLQGIAILNIPSMHGGSNLWGESKKKRSHRR-IEKKGSDKRPTLTD     696
DGKgA|P49620|575-749      ELECDGVEVDLSNIFLEGIAILNIPSMYGGTNLWGETKKNRAVIR-E------SRKSVTD     686
                           :*  *  :** :: *:***:******:**:****::*: :.               :**

DGKaA|P51556|512-693      PDILKTCVPDMSDKRLEVVGIEGVIEMGQIYTRLKSAGHRLAKCSEITFQTTKTLPMQVD     690
DGKbA|P49621|579-759      AKELKFASQDLSDQLLEVVGLEGAMEMGQIYTGLKSAGRRLAQCSSVVIRTSKSLPMQID     756
DGKgA|P49620|575-749      PKELKCCVQDLSDQLLEVVGLEGAMEMGQIYTGLKSAGRRLAQCSSVTIRTKKLLPMQVD     746
                           . ** .  *:**: *****:**.:******* *****:***:**.:.::*.* ****:*

DGKaA|P51556|512-693      GEP    693
DGKbA|P49621|579-759      GEP    759
DGKgA|P49620|575-749      GEP    749
                          ***
#  Percent Identity  Matrix - created by Clustal2.1

     1: DGKaA|P51556|512-693  100.00   63.54   66.86
     2: DGKbA|P49621|579-759   63.54  100.00   81.14
     3: DGKgA|P49620|575-749   66.86   81.14  100.00
```

Supplementary Figure 12. **Sequence alignment of type 1 DGK domains containing probe-modified active site lysines detected by activity-based profiling with ATP acyl phosphates**. Multiple protein sequence alignment of the type 1 rat DGK isoforms (DGKa, DGKb, DGKg) using Clustal Omega highlighting the sequence similarity within the conserved "archetypal" DGK superfamily domains; C1A (green), C1B (blue), catalytic (C, orange), and accessory (A, orange) domains. Regions highlighted in yellow indicate detected tryptic peptides containing probe-modified sites (lysine site of binding highlighted in red) while regions in purple indicate predicted tryptic peptide sequences that were not identified but still contain a conserved lysine residue that is available for probe modification.

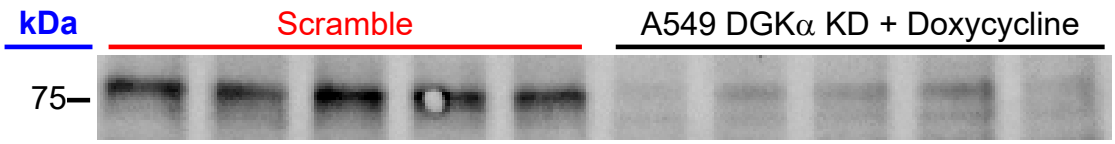

Supplementary Figure 13. **Doxycycline-inducible knockdown of DGKα in non-small cell lung cancer A549 cells**. Western blot displaying shRNA-mediated knockdown (KD) of DGKα in A549 cells following 0.2 μg/mL treatment of doxycycline for 48 hours. A DGKα-specific antibody was used to detect levels of endogenous DGKα (*n*=5 biological samples). Full blot image is shown in Supplementary Fig. 28. Data shown are representative of two experiments (*n*=2 biologically independent samples).

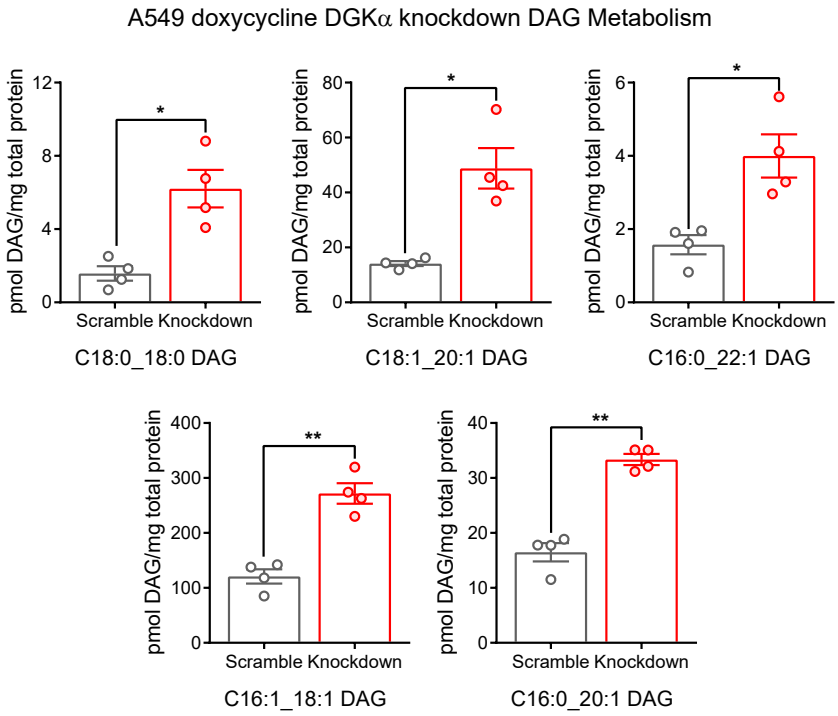

Supplementary Figure 14. **Accumulation of cellular DAGs following shRNA-mediated knockdown of endogenous DGKα in A549 cells**. Knockdown of endogenous DGKα in A549 cells (0.2 μg/mL doxycycline, 48 hours, *n*=4 biological samples) resulted in accumulation of DAG lipids with the indicated fatty acyl composition. Cellular reductions in these same DAG species in gain of DGKα function studies (Supplementary Table 3) support our metabolomics approach for mapping authentic DGK substrates in live cells. Significance of lipid alterations was determined using a Benjamini-Hochberg correction following a two-sided binomial test (*$Q < 0.05$, **$Q < 0.01$). Data shown represents mean ± s.e.m. Data shown are representative of two experiments (*n*=2 biologically independent experiments).

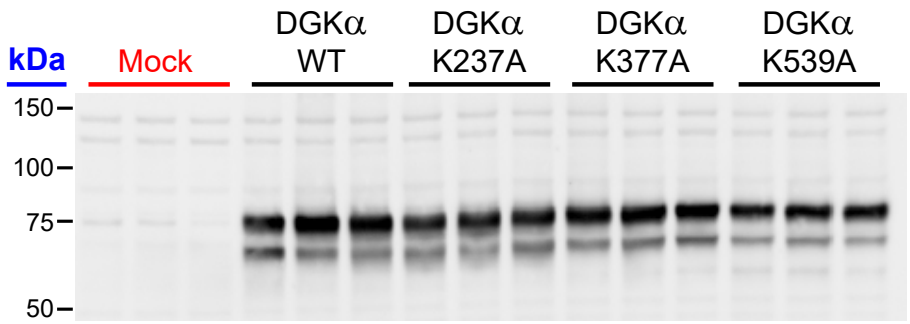

Supplementary Figure 15. **Expression levels of recombinant DGKα wild-type and lysine mutant proteins are comparable**. Western blot showing equivalent expression of wild-type (WT) and lysine-to-alanine mutants of rat DGKα. Lysines selected for mutation are those identified by chemical proteomic analyses with ATP acyl phosphates shown in Fig. 3. Recombinant WT and mutant DGKα expression levels were detected and compared by western blot analysis with an anti-FLAG antibody (*n*=3 biological samples). Full blot image is shown in Supplementary Fig. 29. Data shown are representative of two experiments (*n*=2 biologically independent experiments).

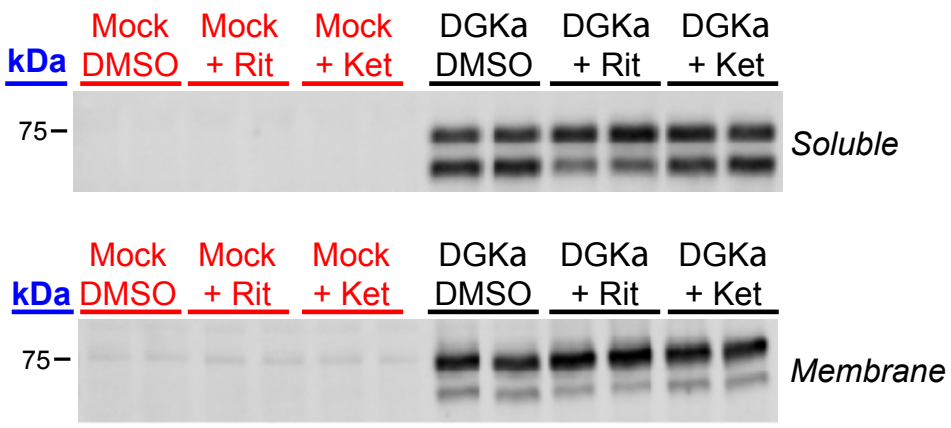

Supplementary Figure 16. **Treatment with small molecule inhibitors does not affect expression levels of recombinant DGKα in cells**. Western blot showing equivalent expression of recombinant rat DGKα in overexpressing HEK293T cells treated with DMSO vehicle, ritanserin (Rit), or ketanserin (Ket, 25 μM compounds, 1 hour, *n*=2 biological samples). Soluble and membrane fractions are shown. Detection was achieved using an anti-FLAG antibody. Full blot image is shown in Supplementary Fig. 30. Data shown are representative of two experiments (*n*=2 biologically independent experiments).

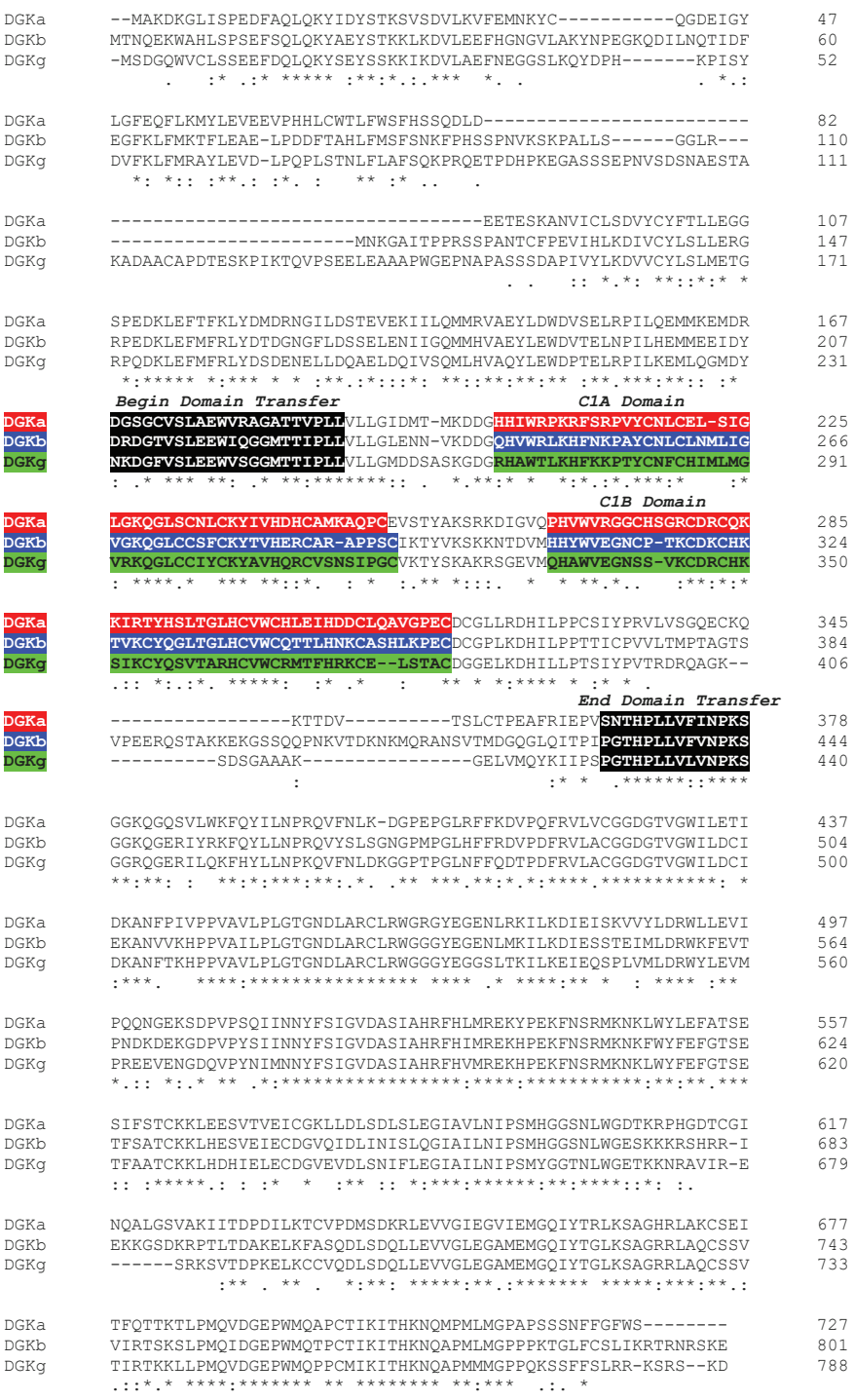

Supplementary Figure 17. **Sequence alignment of type 1 DGK isoforms**. Multiple protein sequence alignment (Clustal Omega) of rat type 1 DGKs to identify homologous regions for C1 domain swaps by protein engineering. Highlighted amino acid sequences denote key locations used for generation of the C1 chimera proteins; black = region enclosing the C1 domain swap, red = DGKα C1 sequences, blue = DGKβ C1 sequences, and green = DGKγ C1 protein sequences.

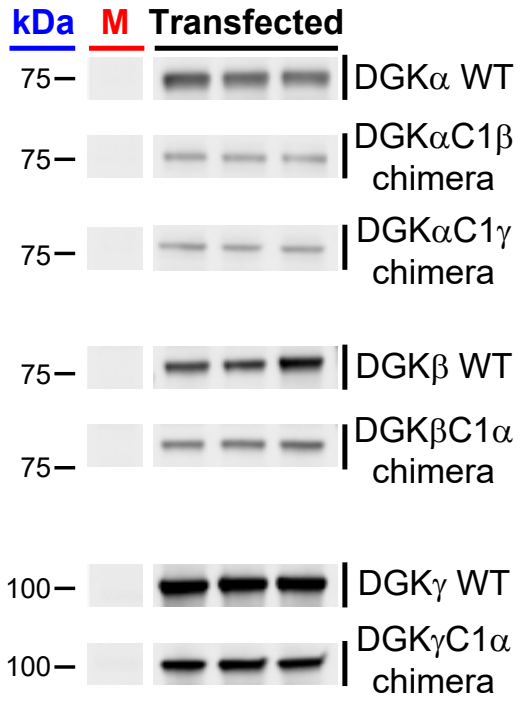

Supplementary Figure 18. **Expression of type 1 recombinant DGK chimeras**. Western blot analysis showing expression of recombinant rat DGK wild-type (WT) and C1 domain chimeras in proteomes from overexpressing HEK293T cells (*n*=3 biological samples). Detection was achieved using an anti-FLAG antibody. Full blot image is shown in Supplementary Fig. 31. Data shown are representative of four experiments (*n*=4 biologically independent experiments).

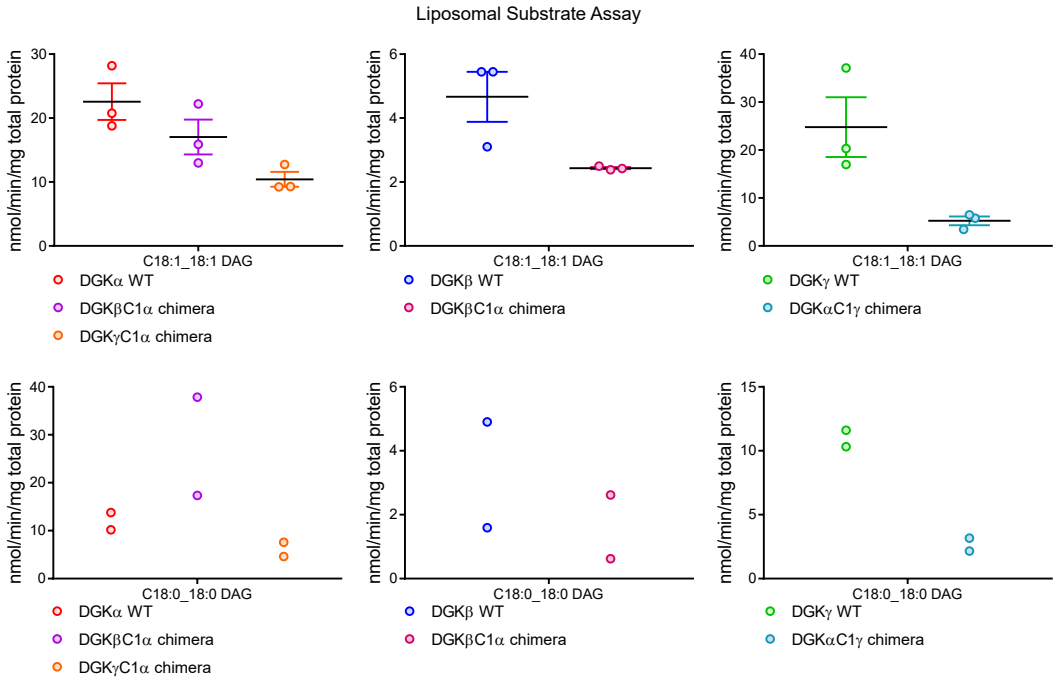

Supplementary Figure 19. **Recombinant DGK chimeras are catalytically active**. Recombinant DGK chimeras are catalytically active as judged by a liposomal substrate assay against both C18:1_C18:1 (*n*=3 biological samples) and C18:0_C18:0 (*n*=2 biological samples) DAG substrate. Liposomes used for substrate assays contained the following composition: 70% DOPC, 20% DOPS, and 10% DAG. Recombinant DGK overexpressed-HEK293T proteomes were used for substrate assays. Data shown represent mean ± s.e.m. Displayed activity (nmol/min/mg total protein) includes subtraction of mock background levels. Data shown are representative of one experiment (*n*=1 biologically independent experiment).

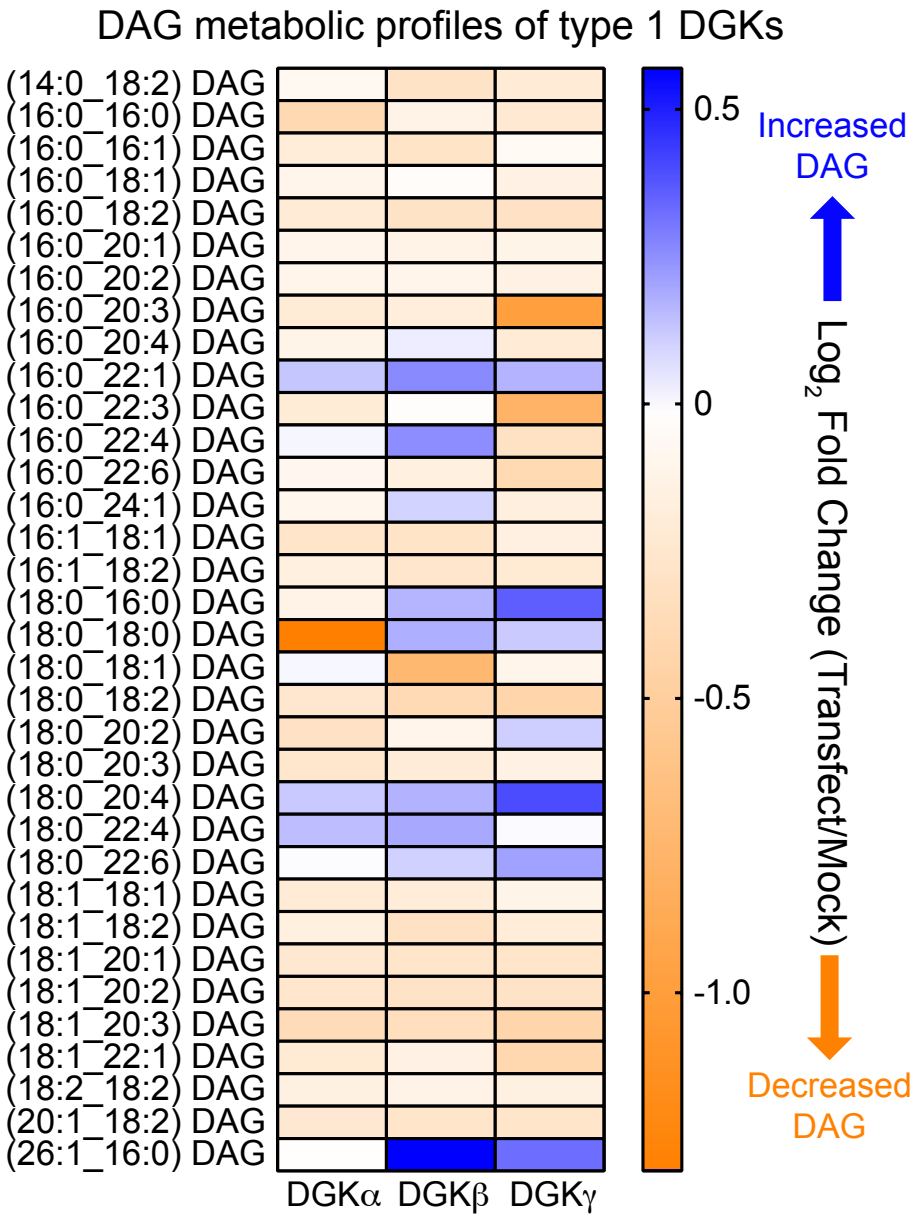

Supplementary Figure 20. **Assigning DAG substrate specificity to type 1 rat DGKs**. Heat map displaying cellular alterations in the DAG lipidome (log_2 fold change) in recombinant rat type 1 DGK overexpressed- compared with mock non-transfected-HEK293T cells (n=6 biological samples). Data shown are representative of two experiments (n=2 biologically independent experiments).

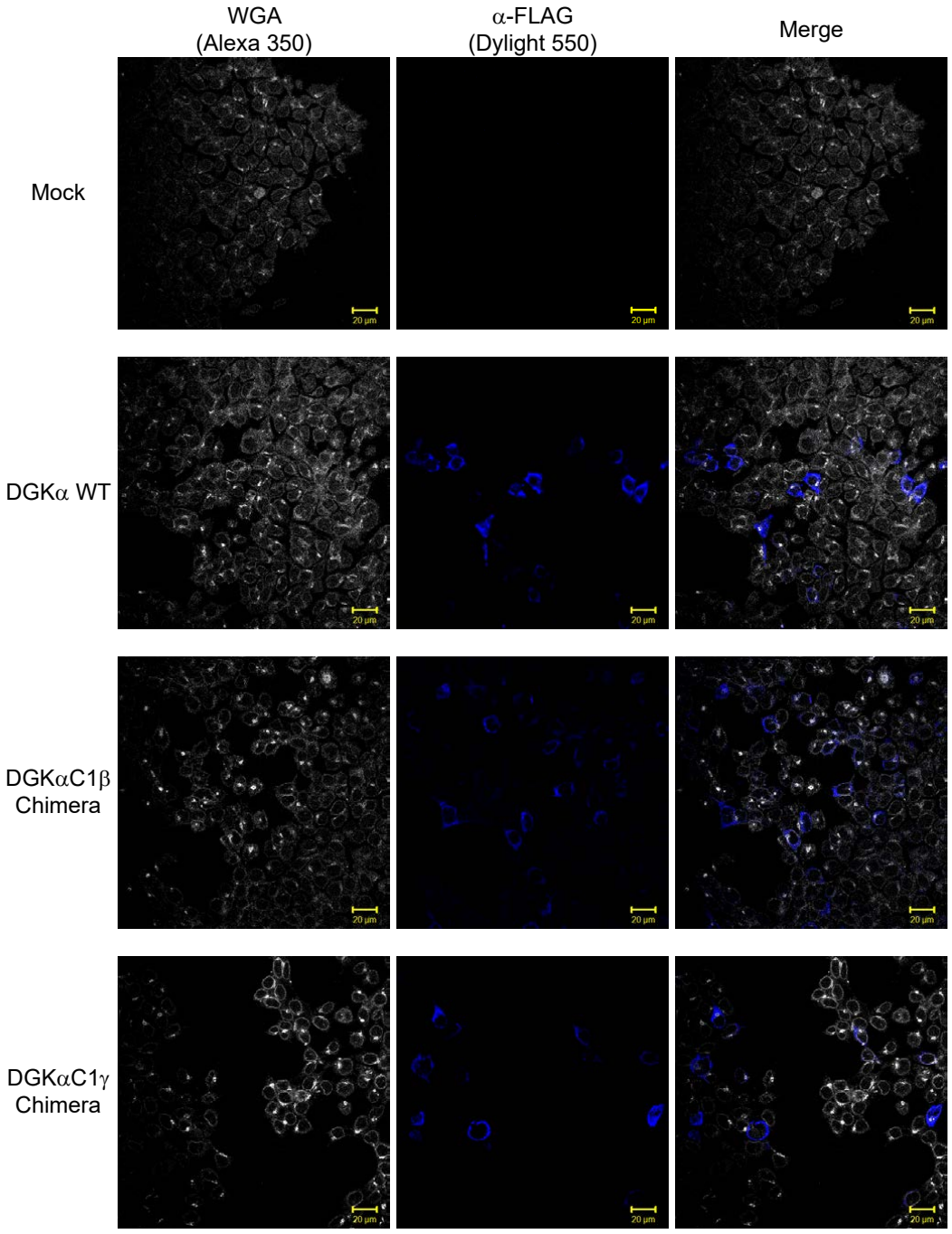

Supplementary Figure 21. **Immunofluorescence analysis of recombinant DGKα and chimeras overexpressed in HEK293T cells**. Images were acquired using a Zeiss 780 NLO Confocal microscope. Membrane staining was accomplished using a wheat germ agglutinin (WGA) conjugated to an Alexa 350 nm fluorophore. Expression of recombinant DGKs (WT and chimeras) was detected using an anti-FLAG antibody. Immunofluorescence did not reveal a clear correlation between subcellular localization of DGK chimera and the WT isoform from which C1 domains were derived. Scale bars are set at 20 µm. Data shown are representative of two experiments (n=2 biologically independent experiments).

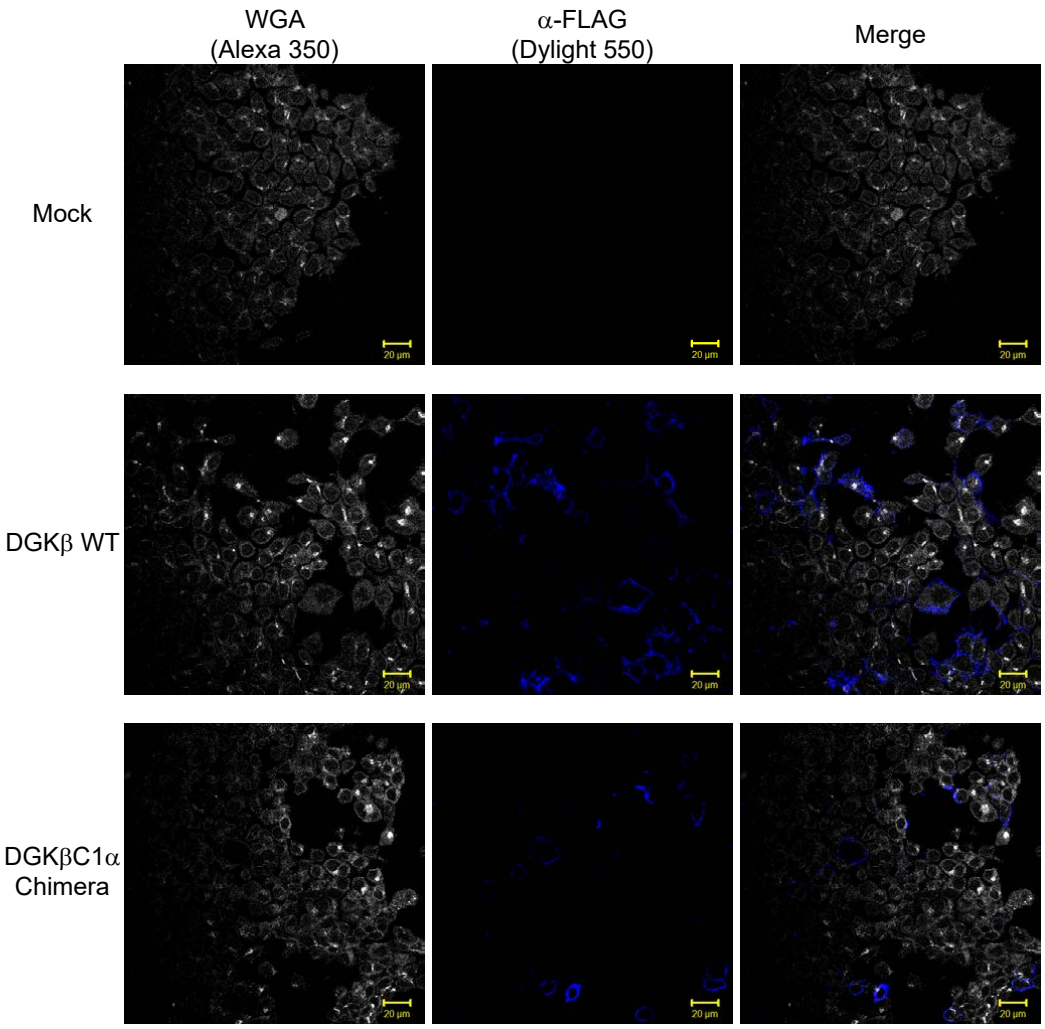

Supplementary Figure 22. **Immunofluorescence analysis of recombinant DGKβ and chimera overexpressed in HEK293T cells**. Experimental conditions for data shown are described in Supplementary Fig. 21. Data shown are representative of two experiments (*n*=2 biologically independent experiments).

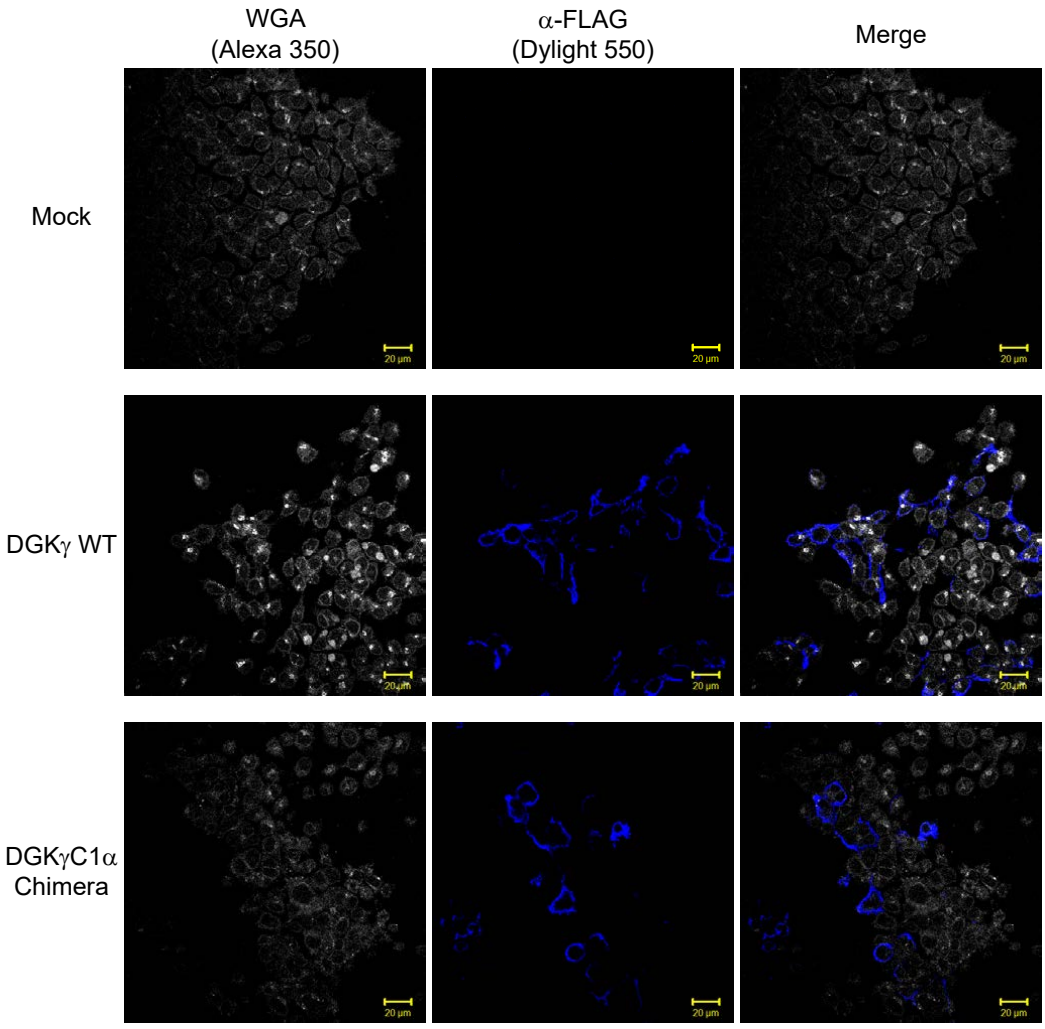

Supplementary Figure 23. **Immunofluorescence analysis of recombinant DGKγ and chimera overexpressed in HEK293T cells**. Experimental conditions for data shown are described in Supplementary Fig. 21. Data shown are representative of two experiments (*n*=2 biologically independent experiments).

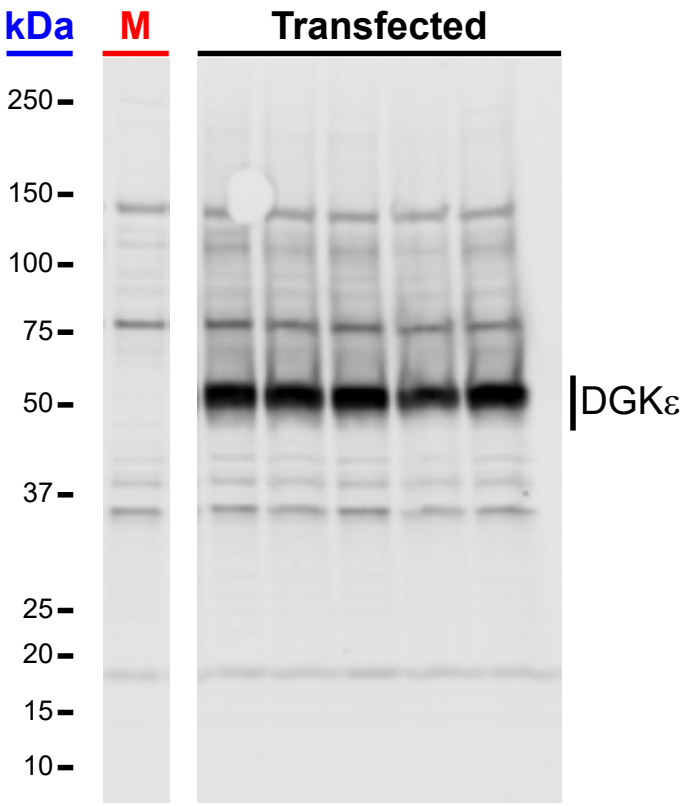

Supplementary Figure 24. Full images of blots related to Fig. 1d.

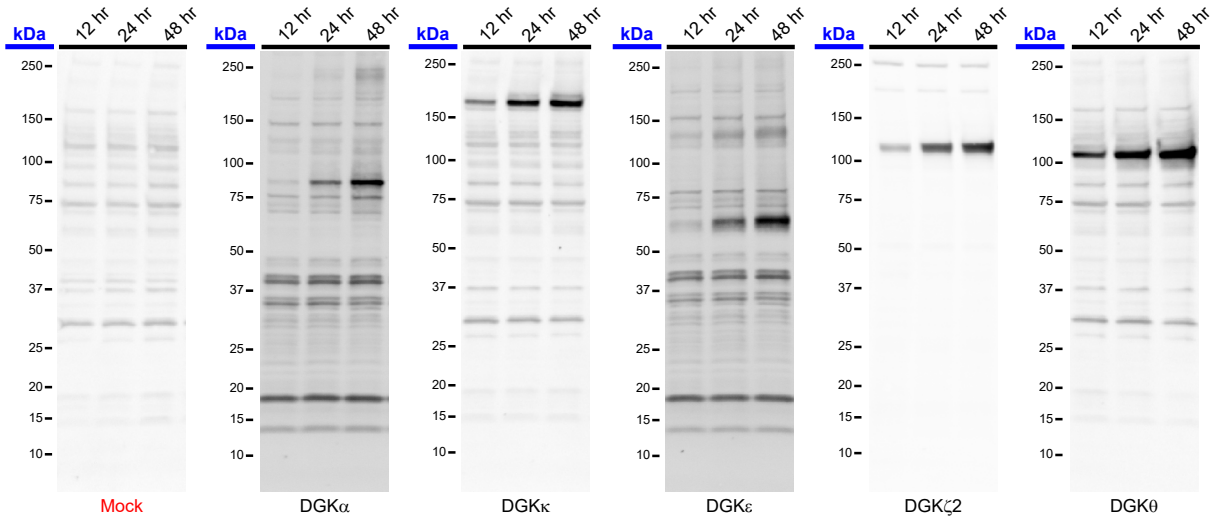

Supplementary Figure 25. Full images of blots related to Supplementary Fig. 3.

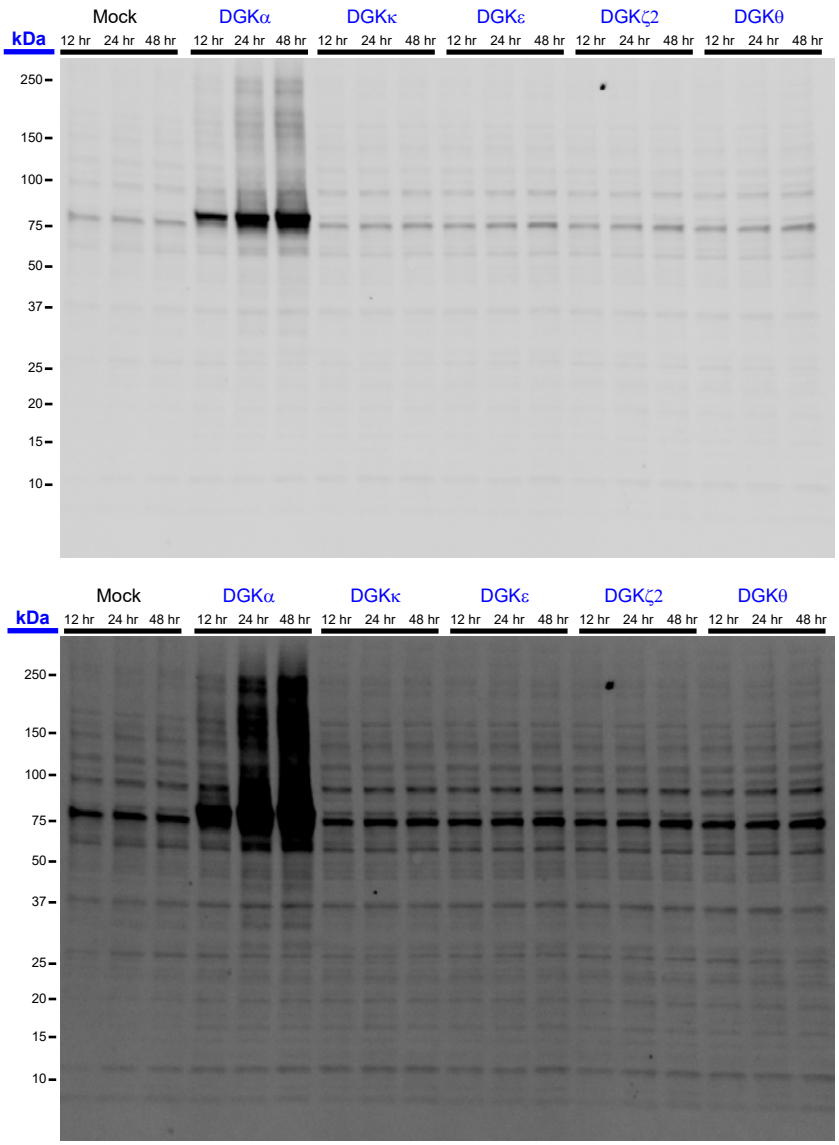

Supplementary Figure 26. Full images of blots related to Supplementary Fig. 4.

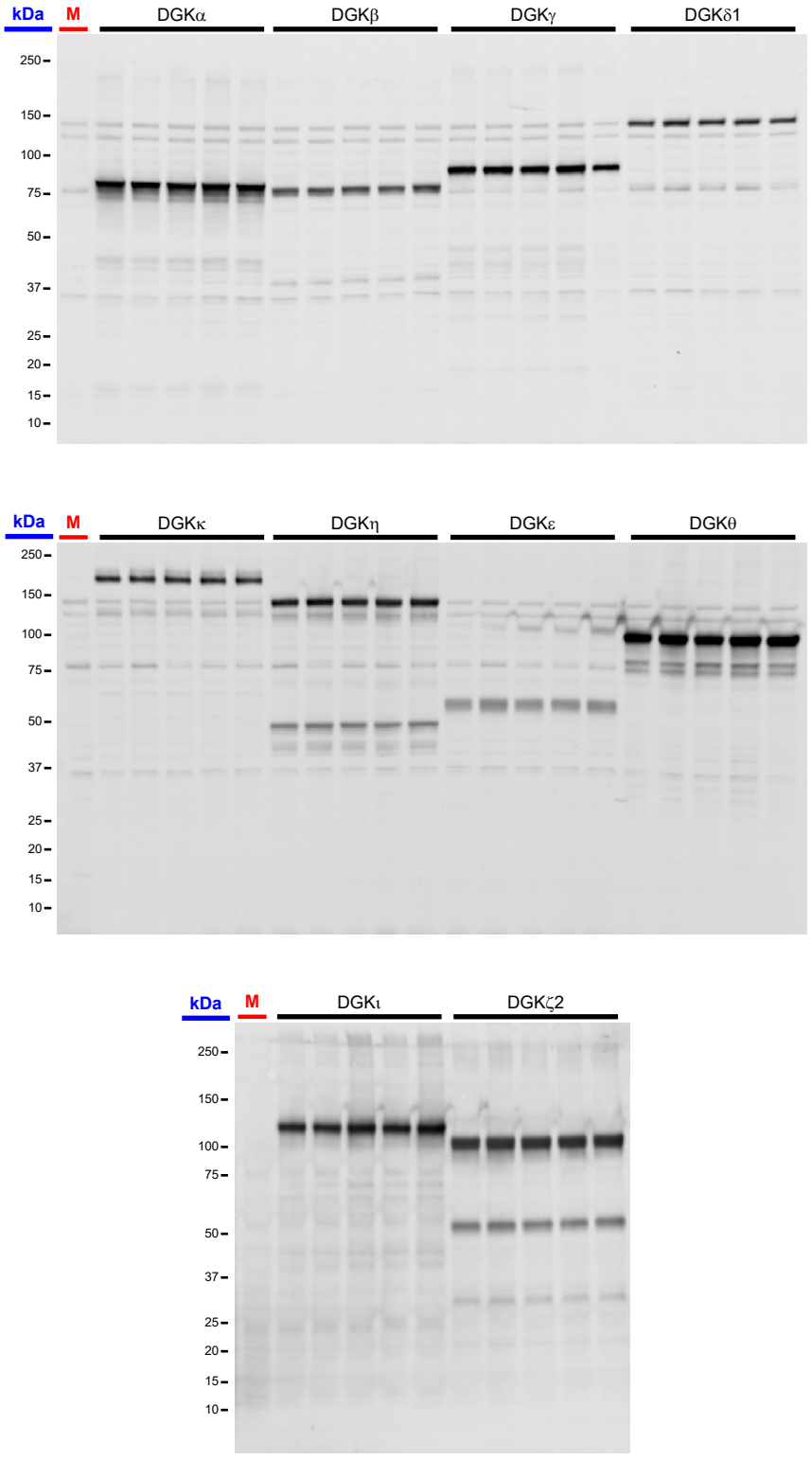

Supplementary Figure 27. Full images of blots related to Supplementary Fig. 7.

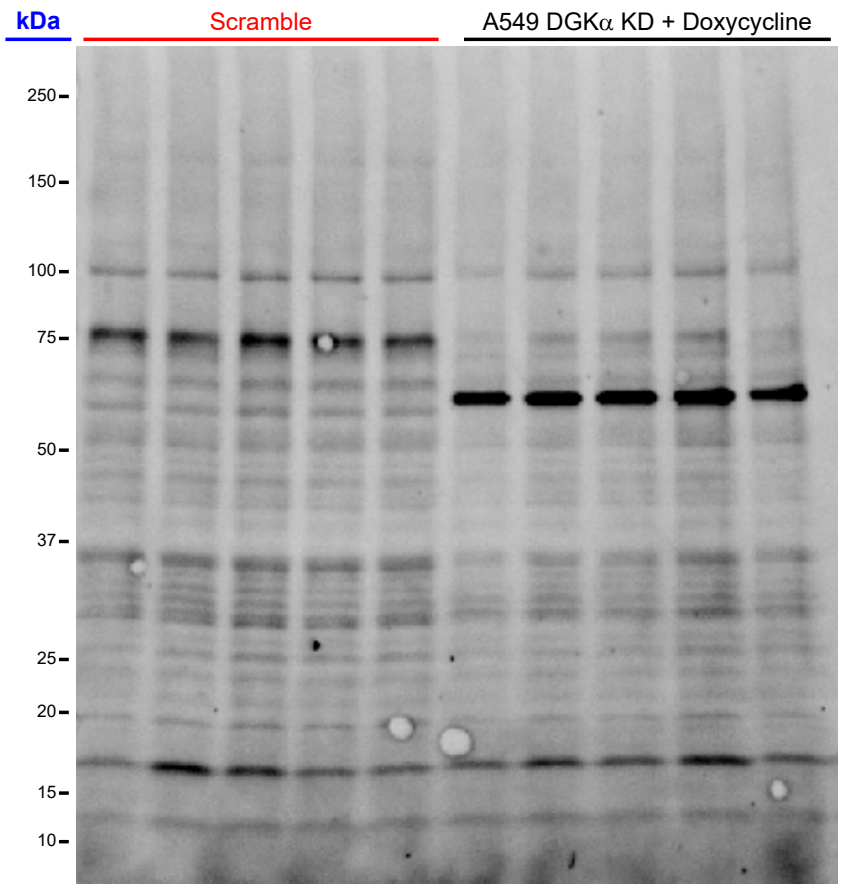

Supplementary Figure 28. Full images of blots related to Supplementary Fig. 13.

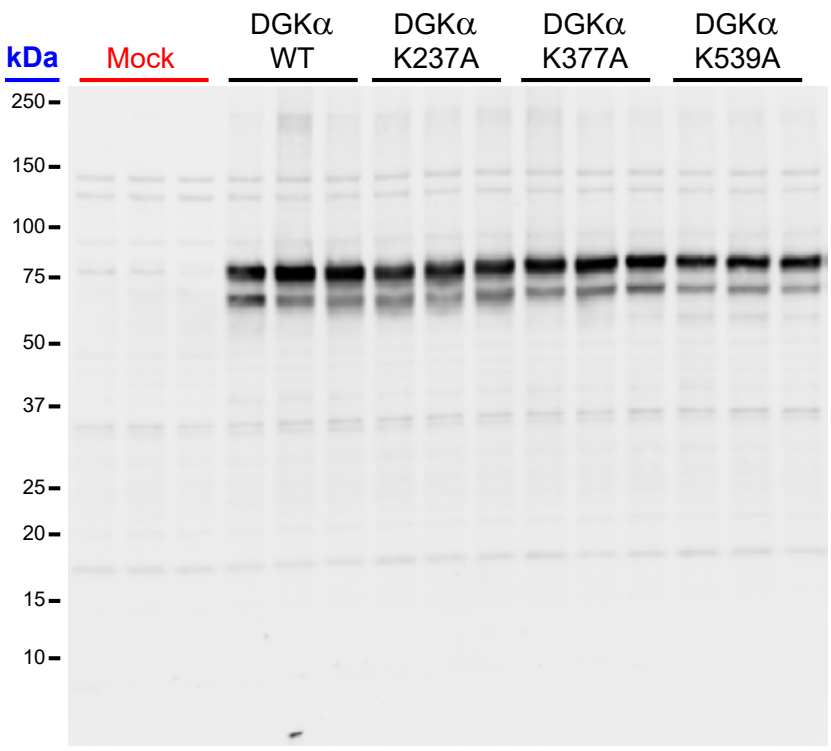

Supplementary Figure 29. Full images of blots related to Supplementary Fig. 15.

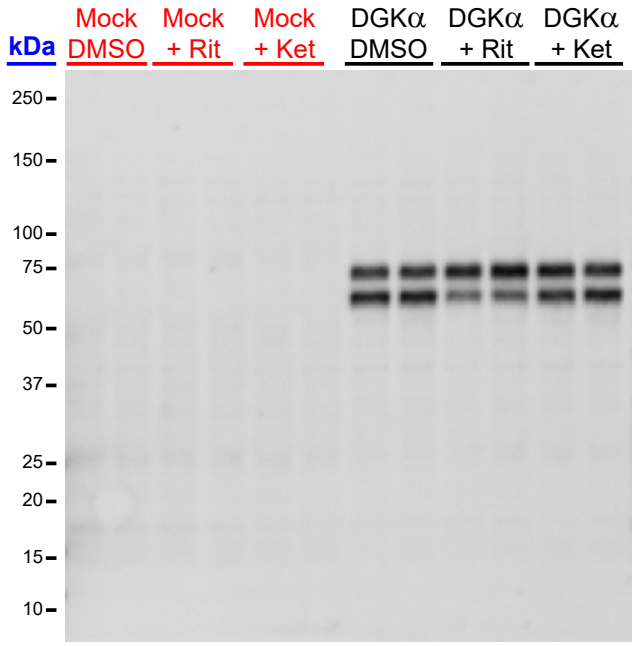

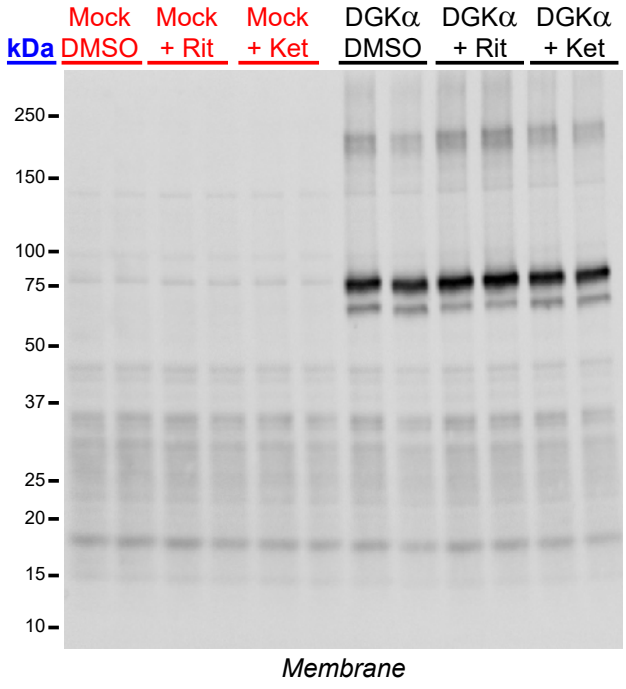

Supplementary Figure 30. Full images of blots related to Supplementary Fig. 16.

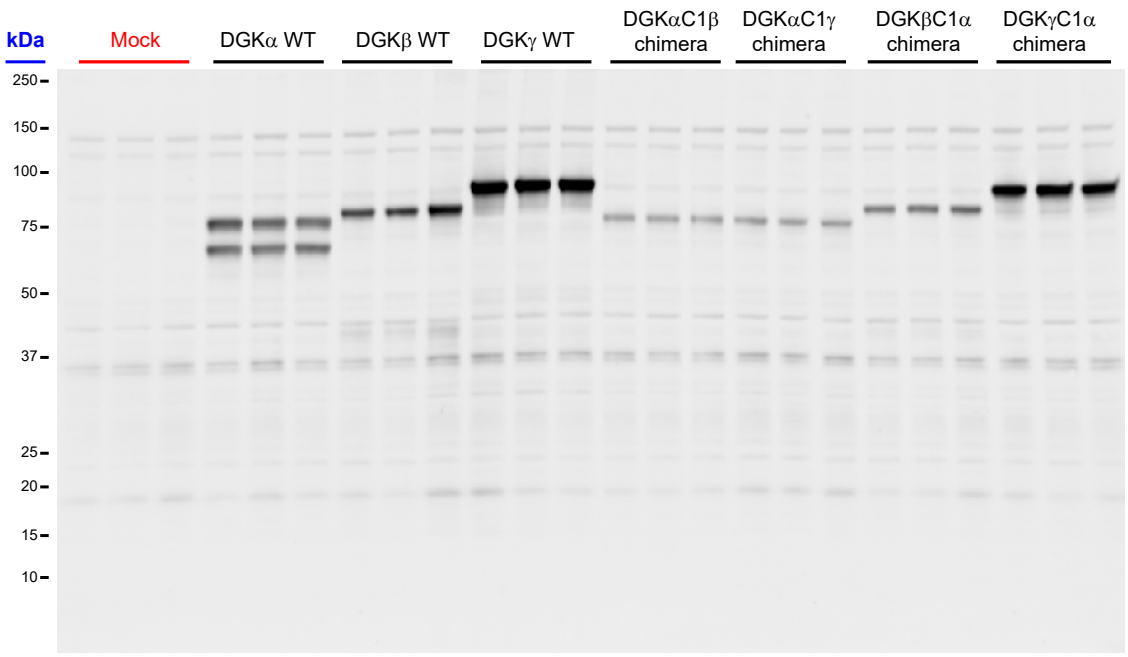

Supplementary Figure 31. Full images of blots related to Supplementary Fig. 18.

SUPPLEMENTARY DATASETS

Supplementary Dataset 1.

A) Results from LipidSearch analysis of both positive and negative mode ddMS2 data from DGKε overexpressed HEK293T lipidomes. Job results for identified lipid species are filtered as outlined in Supplementary Figure 5. Data displayed are used to generate Fig. 1b.

B) Abundances of identified DAG species from DGKε overexpressed HEK293T lipidomes following a targeted PRM analysis identifying the NH_4^+ adduct. Normalization is accomplished using the detected SAG-d8 internal standard and protein concentration. Data displayed is used to generate Fig. 1d.

C) Log_2 fold changes of DAG abundances from various DGK isoforms overexpressed in HEK293T cells. All DGK isoforms are the human variant. Data displayed is used to generate Fig. 2a and b and Supplementary Fig. 8, 9 and 11.

D) SILAC ratios and modified peptides of soluble proteins from DMSO (light)/ATP (heavy) treatments of HEK293T cells overexpressed with type 1 rat DGK isoforms with the ATP acyl phosphate probe. Data displayed is used to generate Fig. 3.

E) Abundances of identified DAG species from type 1 human DGK isoform overexpressed HEK293T lipidomes following a targeted PRM analysis identifying the NH_4^+ adduct. Data displayed is used to generate Fig. 4a.

F) Abundances of identified DAG species from A549 lipidomes following doxycycline-induced shRNA knockdown of DGKα. Data displayed is used to generate Fig. 4b.

G) Abundances of identified DAG species from rat DGKα WT and lysine mutant overexpressed HEK293T lipidomes following a targeted PRM analysis identifying the NH_4^+ adduct. Data displayed is used to generate Fig. 4c.

H) Abundances of identified DAG species from rat DGKα WT overexpressed HEK293T lipidomes treated *in situ* with ritanserin and ketanserin. Data displayed is used to generate Fig. 4d.

I) Abundances of identified DAG species from type 1 rat DGK WT and C1 chimera overexpressed HEK293T lipidomes following a targeted PRM analysis identifying the NH_4^+ adduct. Data displayed is used to generate Fig. 5.

J) Log_2 fold changes of PA abundances from various DGK isoforms overexpressed in HEK293T cells. All DGK isoforms are the human variant. Data displayed is used to generate Supplementary Fig. 10 and 11.

K) Phosphorylation activity studies of type 1 DGK WT and chimera isoforms overexpressed in HEK293T soluble proteomes. Formation of radiolabeled [γ^{32}-P] PA product is used to determine *in vitro* DGK activity from liposome substrates. Data displayed are used to generate Supplementary Fig. 19.

L) Log_2 fold changes of DAG abundances from type 1 DGK isoforms overexpressed in HEK293T cells. All DGK isoforms are the rat variant. Data displayed are used to generate Supplementary Fig. 20.